Journal Pre-proof

A Probabilistic Framework for Post-Disaster Recovery Modeling of Buildings and Electric Power Networks in Developing Countries

Eyitayo A. Opabola , Carmine Galasso

PII: S0951-8320(23)00593-8
DOI: https://doi.org/10.1016/j.ress.2023.109679
Reference: RESS 109679

To appear in: *Reliability Engineering and System Safety*

Received date: 26 March 2023
Revised date: 7 September 2023
Accepted date: 21 September 2023

Please cite this article as: Eyitayo A. Opabola , Carmine Galasso , A Probabilistic Framework for Post-Disaster Recovery Modeling of Buildings and Electric Power Networks in Developing Countries, *Reliability Engineering and System Safety* (2023), doi: https://doi.org/10.1016/j.ress.2023.109679

Highlights

- Recovery modeling framework capturing technical, socioeconomic, and political factors
- Integration of recovery trajectories of utility networks and residential buildings
- Inclusive post-disaster intervention prioritisation using an optimization algorithm
- Data-driven recovery time model for electric power networks in developing countries

A Probabilistic Framework for Post-Disaster Recovery Modeling of Buildings and Electric Power Networks in Developing Countries

Eyitayo A. Opabola[1] **and Carmine Galasso** [1]

Department of Civil, Environmental and Geomatic Engineering, University College London, United Kingdom

ABSTRACT

Post-disaster recovery is a significant challenge, especially in developing countries. Various technical, environmental, socioeconomic, political, and cultural factors substantially influence post-disaster recovery. As a result, methodologies relevant in developed nations may not be directly applicable in Global South contexts. This study introduces a probabilistic framework for modeling the post-disaster recovery of buildings and electric power networks (EPN) in developing countries. The proposed framework combines a building-level assessment of individual assets with a community-level assessment of EPNs to evaluate a building portfolio's post-event functionality state. As part of the framework, a stochastic network analysis approach is proposed to estimate the recovery time of damaged buildings while accounting for technical, environmental, socioeconomic, political, and cultural factors, quantified using data gathered from past events. Similarly, a probabilistic modeling approach is proposed to quantify the EPN's initial post-event outage levels. Specifically, empirical formulations for estimating the recovery time of an EPN as a function of its initial post- event outage levels are calibrated using post-event data from developing countries. A case study is presented to illustrate the application of the proposed framework to model the post-earthquake recovery of a synthetic low-income residential community. The analysis showed that negative technical, environmental, socioeconomic, political, and cultural factors could amplify the reconstruction time of damaged buildings by a factor of almost three. The proposed framework can support decision-makers in disaster planning and management strategies for vulnerable low-income communities.

Keywords: post-earthquake recovery, developing countries, resilience, electric power networks, decision support

1 INTRODUCTION

Recent catastrophic events worldwide have emphasized the challenges to achieve rapid post-disaster recovery, particularly in Global South contexts. For example, the majority of the occupants of the over 500,000 buildings demolished after the 2015 Gorkha earthquake continued to live in temporary shelters for over 18 months after the disaster (The Asia Foundation 2016). About 65,000 displaced people were still homeless five years after the 2010 Haiti earthquake (IOM 2015). The delayed recovery process in some of these countries, especially low-income ones, is often influenced by various technical, environmental, socioeconomic, political, and cultural aspects (e.g., the presence of political conflicts or war, availability of stable governance, land disputes, and lack of technical know-how, among many other factors (Chang et al. 2011; Sharma et al. 2018; Weerakoon et al. 2007).

This study focuses on developing countries as defined by the United Nations Development Programme's Human Development Index, which is based on Gross National Income, life expectancy, and education level (UNDP 2021). Recovery modeling frameworks available in the literature are either building-specific or community-level. Regarding building-level post-disaster recovery modeling, various studies (e.g., Almufti and Willford 2013; Cook et al. 2022; Terzic et al. 2021)) have been developed to evaluate the downtime and recovery trajectory of damaged buildings. However, these studies focus mainly on repair downtime modeling. Therefore, they may be unable to capture long-term recovery facets of low-income countries typically dominated by reconstruction and not repair. Furthermore, these studies do not consider the diversity in disaster resilience between countries due to various geographic, technical, environmental, socioeconomic, political, and cultural factors. As such, some of the existing frameworks may not be easily extrapolated to regions outside of the regions for which they were developed, for instance. Similar conclusions can be reached for most community-level recovery modeling studies (e.g., Aghababaei et al. 2020; Aghababaei and Koliou 2022; Lin and Wang 2017a; Wang and van de Lindt 2021) focusing on developed nations. It is noted that studies (e.g., Burton et al. 2017) have developed post-disaster housing frameworks that implicitly consider socioeconomic factors. However, existing studies lack a harmonized framework to adequately account for the previously mentioned factors that strongly influence recovery processes in developing countries. This is a research gap that needs to be filled.

Several studies have been carried out on post-disaster recovery modeling and resilience assessment of lifeline systems. For example, post-disaster resilience modeling frameworks of water networks have been proposed in research studies (e.g., Chang and Shinozuka 2004; Liu et al. 2020). Research studies (e.g., Kammouh et al. 2020; Li et al. 2019; Pan et al. 2022; Wu and Chen 2023; Yu and Gardoni 2022; Zou and Chen 2021) have investigated the post-disaster resilience of transportation networks. Both water and transport networks are outside the scope of this specific study.

Research studies (e.g., Barabadi and Ayele 2018; Mensah and Dueñas-Osorio 2016; Ouyang and Dueñas-Osorio 2014; Unnikrishnan and van de Lindt 2016) have also investigated and developed post-disaster probabilistic resilience assessment frameworks for electric power networks (EPNs). To account for the fact that disaster-induced disruptions in one network (e.g., transportation) may result in disruptions to other networks and lead to their reduced functionality and/or affect their recovery, studies (e.g., Almoghathawi et al. 2023; Danziger and Barabási 2022; Dueñas-Osorio and Kwasinski 2012; Guidotti et al. 2016; He and Cha

2018; Johansen and Tien 2018; Sharma and Gardoni 2022; Xiao et al. 2022) have proposed probabilistic recovery modeling of dependent/interdependent infrastructure networks. Critical gaps in these studies include: (1) existing studies focus on developed countries; (2) the majority of the studies are typically community-level (i.e., regional) studies and do not quantify the impact of utility outages on the functionality and recovery of individual buildings; and (3) the recovery models for lifeline systems do not consider important socioeconomic, political, and cultural factors (either directly or indirectly).

Based on these remarks, the current study proposes a framework for post-disaster recovery modeling of disaster-struck marginalized communities in low and lower-middle-income countries with appropriate consideration of the influence of community-level electric power outages on the recovery pathways of buildings. Firstly, using data from past events, the study highlights critical socioeconomic, political, and cultural factors that can impede or speed up post-disaster recovery. Subsequently, a post-disaster functional recovery modeling framework is presented. The proposed framework combines a building-level assessment of their structural and nonstructural seismic performance with a community-level assessment of the EPN serving those buildings. The novel aspects of the proposed framework include (a) contributing to inclusive recovery simulation through incorporating a multicriteria decision-making approach (that captures the influence of technical, socioeconomic, political, environmental, and cultural factors) for community-level intervention sequencing in a recovery modeling framework; (b) developing a stochastic network analysis approach for estimating the recovery time of damaged buildings, using historical data-driven recovery time amplification and mitigation factors; (c) developing empirical formulations (based on historical data) to predict the community-level recovery time of power networks as a function of initial post-disaster outage level; and (d) the development of an approach for simulating historical recovery trajectory scenario on EPNs. Finally, a case study is presented to demonstrate the applicability of the proposed framework to model the post-earthquake recovery of a residential community. The proposed framework can serve as a tool to inform decision-makers on disaster planning and management strategies. For example, local authorities can use information from recovery trajectories to manage short-term and long-term shelter needs, among other issues.

2 FACTORS INFLUENCING POST-DISASTER RECOVERY

Compared to pre-disaster construction projects, post-disaster recovery projects are generally more complex, dynamic, and chaotic (e.g., Davidson et al. 2007). Different post-disaster recovery programs in different countries have unique features that can influence recovery (Comerio 2016). Due to the impact of various factors, post-disaster reconstruction projects in developing countries can take several years. For example, the reconstruction of about 40,000 housing units following the 1999 Izmit earthquake took over six years (Tas et al. 2011). Reconstruction projects are still ongoing in Central Sulawesi five years after the 2018 earthquake and tsunami.

A key objective of this study is to quantify the impact of various factors affecting post-disaster recovery time overrun for numerical simulation purposes. First, a literature review was conducted to identify the quantified impacts of various recovery-impeding factors on task completion duration for post-disaster recovery projects. Second, data from stakeholder engagements with engineers, contractors, government and non-government agency officials, and disaster victims involved in the recovery process of residential and school buildings following the 2018 Central Sulawesi earthquake and tsunami were adopted. The stakeholder engagements were in the form of surveys, semi-structured interviews and workshops. Opabola et al. (2023) provide more information on the stakeholder engagements.

From both tasks (i.e., literature review and stakeholder engagement), eight critical factors were identified and classified: hostile political conditions (socioeconomic/political factor), land dispute issues (socioeconomic factor), epidemic-induced delays (environmental factor), delays associated with material procurement (socioeconomic), poor management skills (technical), delays in funds disbursement (socioeconomic), technical delays (technical), and community participation (socioeconomic). It is noted that other factors may impact recovery. However, this paper focuses on the prominent and quantified factors from our study.

Hostile political conditions have been reported to amplify post-disaster recovery time in developing/low-income countries. Such conditions include the absence of local government officials to coordinate the recovery process (Sharma et al. 2018), political instability and conflicts (Samaratunge et al. 2012), and bureaucratic burdens, egoism, vested interests and corruption among government officials (Sharma et al. 2018). For example, Sharma et al. (2018) reported that due to the absence of local government officials, resolving fundamental issues (e.g., tender process, building permits, and land acquisition) took at least four times the ideal time following the 2015 Gorkha earthquake. Also, data presented by Weerakoon et al. (2007) show that the recovery rate of buildings in Sri Lanka following the 2004 Indian Ocean tsunami was up to eight times larger in conflict zones compared to zones outside the conflict region (Figure 1). In Sri Lanka, conflicts influenced post-disaster recovery time by a factor of about five. Furthermore, empirical construction delay prediction models (e.g., Gondia et al. 2020) show that, even without disasters, hostile political conditions amplify construction project time by at least 60%. Based on this evidence, this study assumes a range of 1.5 to 5 as time amplification factors due to hostile political conditions.

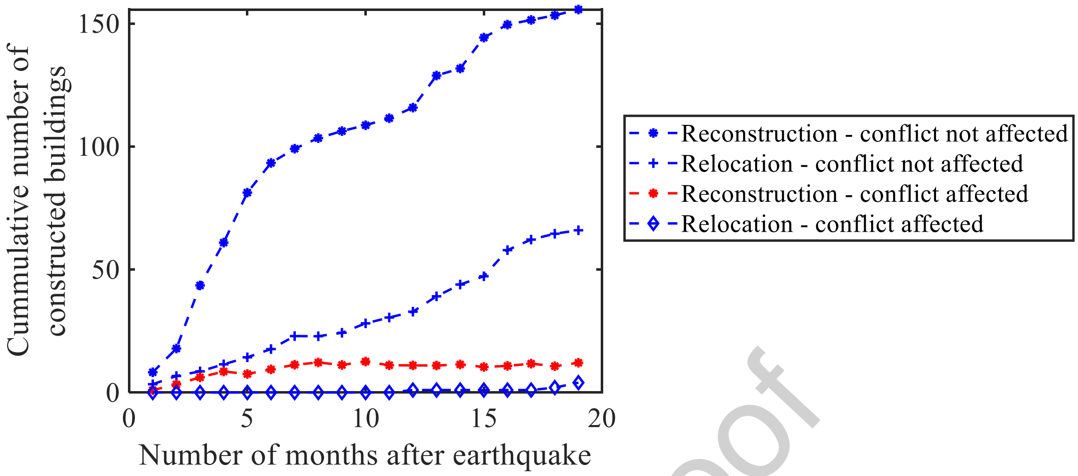

Figure 1 – Influence of conflict and recovery type on recovery projects of residential buildings following the 2004 Indian Ocean tsunami (Data from Weerakoon et al. (2007))

Land dispute resolutions are typically relevant for relocation projects. After a significant event, the government typically enforces a ‘no build’ zone (or multiple of those). For instance, the Sri Lankan government introduced 100m and 200m coastal buffer zones in the south and east after the 2004 Indian Ocean tsunami to restrict reconstruction. As a result, people in such regions needed to be relocated to other sites. Delays on such relocations could take several months (Weerakoon et al. 2007). Data from the post-2010 Haiti earthquake (Jahn et al. 2017) show that land rights issues amplified reconstruction time by a factor of up to two. Waheeb and Andersen (2022) have also reported that land disputes resulted in post-disaster reconstruction time overrun with factors ≥ 1.25 in Iraq.

Post-disaster reconstruction projects are either community-/owner-managed or agency-managed (Karunasena and Rameezdeen 2010). Various literature (e.g., Westoby et al. 2021) has highlighted the significant delays in the tender selection process and contract award associated with agency-managed projects. Opabola et al. (2023) observed delays in agency-managed projects which were partly attributed to poor management situations where contracts were awarded to the lowest bidder, who may not necessarily have the best experience/know-how to plan and manage the project accordingly. By comparing the reconstruction times of community-/owner-managed and agency-managed following the 2018 Central Sulawesi earthquake and tsunami from stakeholder engagement, it is observed that tasks in community-/owner-managed projects were completed at least 1.45 times faster than tasks in agency-managed projects. Waheeb and Andersen (2022) have attributed time overrun factors of up to three to poor management.

Increased construction material costs have been reported following major global earthquakes and other catastrophic events. The increased cost is due to demand surge and supply shortage associated with increased material transportation costs, inadequate production capacity, local material scarcity, and profit-driven price gouging by suppliers (e.g., ADB 2007; AIR 2021; Chang et al. 2011). To optimize budget, construction projects are typically delayed until material costs have stabilized, potentially leading to significant delays. ADB (2009) reported that the post-disaster reconstruction rate in Aceh was about 2.3 times slower than expected.

Community/stakeholder participation during the recovery planning and implementation phases has been reported to reduce post-disaster recovery time (e.g., Ophiyandri et al. 2013; Shafique and Warren 2015; Tas et al. 2011). Reports (e.g., Gharaati and Davidson 2008; Kennedy et al. 2008; Tas et al. 2011) have highlighted that poor community engagement can lead to construction delays, rejection by beneficiaries, and rework of newly constructed buildings. Based on reports from the aforementioned literature and stakeholder engagements in Central Sulawesi, recovery tasks that benefitted from community participation were observed to have been completed 10-30% faster.

Based on the discussions presented above, Table 1 provides ranges of amplification and mitigation factors that can be used for post-disaster recovery time modeling in developing countries. Only one time overrun multiplier could be sourced from existing literature for certain factors (e.g., delay in material procurement). In such cases, the identified multiplier is treated as an upper-bound while the lower bound is based on the authors' judgement. The multipliers for technical delays are based on Waheeb and Andersen (2022) and Gondia et al. (2020). The time overrun multipliers attributed to pandemics are based on reported differences in construction task completion in pre- and mid-COVID-19 scenarios (nPlan 2022; Opabola et al. 2023). The subsequent sections of this study introduce a post-disaster recovery framework and propose a methodology for incorporating the time overrun multipliers in recovery time simulation.

Table 1 –Factors for modeling recovery times

Parameter	Time overrun multiplier
Time amplification factors	
Land dispute resolution	1.25 – 2
Pandemic*	1.5 – 3
Delay in material procurement	1.2 – 2.5
Hostile political conditions	1.5 – 5
Poor management skills	1.5 – 3
Funds disbursement	1.25 – 3
Technical delays	1.2 – 2.5
Time mitigation factor	
Community participation	0.5 – 0.9

* Peak values are specified for time-dependent factors (discussed in Section 3.7)

3 PROPOSED FRAMEWORK

3.1 Overview

The proposed post-disaster recovery modeling framework combines community-level functionality estimates for EPNs with building-level functionality estimates of individual buildings to evaluate the recovery trajectory of a disaster-hit community (Figure 2). As shown in the figure, there are five distinct modules in the proposed framework – hazard analysis, post-event functionality assessment, decision-making analysis, intervention prioritization analysis, and recovery time analysis. The hazard analysis is used to generate hazard-induced intensity measures (IMs) (e.g., peak ground accelerations and spectral accelerations in the case of earthquake hazard) at each building site and location of the components and systems within the EPNs (Section 3.2). Power outage assessment at each building site relies on the available information on the generation, transmission, and distribution networks (e.g., fragility functions and connectivity). The post-event functionality of each building is estimated based on the building's damage state and the availability of power supply (see Section 3.2). The study does not focus on water networks, as evidence shows that several low-income communities rely on local wells for water sources. In addition, the link between the recovery of the transport network and residential buildings is outside this study's scope. Once the post-event functionality level of each building is assessed, the decision-making module (described in section 3.3) is used to identify the appropriate intervention for each building. It is noted that both the post-event functionality level assessment and decision-making analysis are building-level analyses.

To ensure inclusive recovery, this study proposes an intervention prioritization module (described in section 3.4) that decision-makers can use to define the intervention hierarchy for each damaged building in the community based on relevant socioeconomic, political, environmental, and cultural factors. The fifth module is the recovery time module, which defines the recovery time for the EPN and the recovery time for each building, accounting for the building's place in the prioritization list (Section 3.7). The recovery time for EPNs (i.e., the time to repair or replace damaged components and systems) can be estimated through simulation-based approaches, which assume an intervention sequence (e.g., Shinozuka et al. 2004). As an alternative, the current study (Section 4.3) proposes empirical formulations for estimating power downtime as a function of the outage level of the EPN, defined through an initial operability assessment (Section 4.2). Furthermore, we propose an approach for estimating the recovery time of each building using time amplification and mitigation factors relevant to low and lower-middle-income communities.

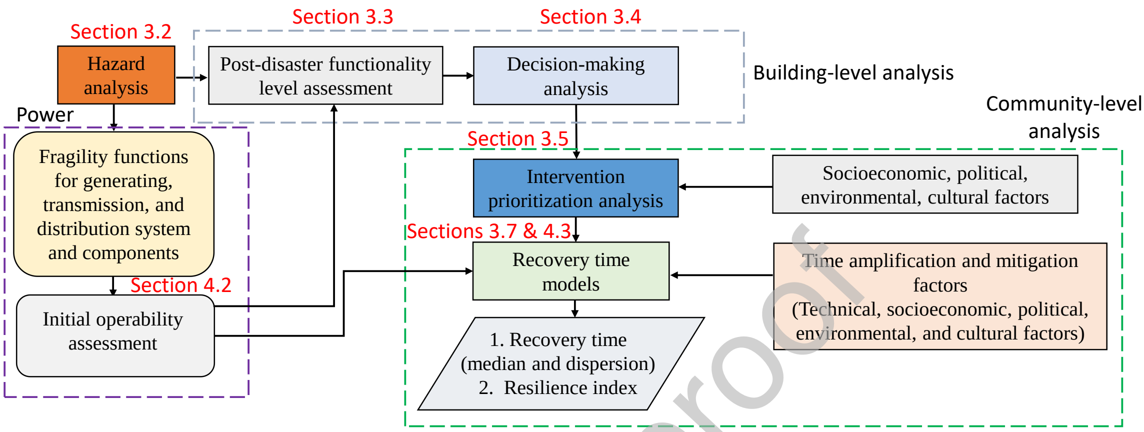

Figure 2 – Proposed framework

3.2 Hazard analysis

In the first part, for a pre-defined event scenario, a hazard analysis to simulate the local hazard intensity measures (e.g., earthquake-induced ground shaking, flood-induced water depth, typhoon-induced wind speeds) at each building site, and location of the components and systems (Campbell and Bozorgnia 2014; Resio et al. 2009; Stewart et al. 2015). The hazard analysis adequately accounts for the spatial distribution of the intensities throughout the region of interest (Huang and Galasso 2019; Kuehn and Abrahamson 2020; Markhvida et al. 2018).

3.3 Post-event functionality assessment

The post-event functionality of a building is dependent on the damage states/levels of its various structural and nonstructural systems and the utility networks (and their components) serving it. Post-event damage assessment of such systems is performed by relating hazard-induced intensity measures (IMs) (e.g., peak ground accelerations and spectral accelerations in the case of earthquake hazard) and/or hazard-induced engineering demand parameters

(EDP) (e.g., interstory drifts and peak floor accelerations) to building-level and/or component-level damage and loss estimates. This is done through fragility models expressing the probability of various building-level damage levels as a function of a hazard IM (e.g., Gautam et al. 2021; Martins and Silva 2021; Giordano et al. 2021) or the probability of various component-level damage levels as a function of an EDP (e.g., FEMA 2012) for both structural and nonstructural components/systems within a building. Similar fragility models can be used for the components of a utility network (e.g., Ang et al. 1996; FEMA 2003; Shinozuka et al. 2007; Straub and Der Kiureghian 2008; Vanzi 2000)).

The functionality level assessment implemented in this study builds on existing building-level functionality assessment approaches (e.g., Lin and Wang 2017b) to classify buildings into four functionality levels (FL0, FL1, FL2, and FL3) based on the damage states of the structural and nonstructural components and utility service availability (See Figure 3 for a description of each functionality level). However, while existing studies (e.g., Lin and Wang 2017b) provide prescriptive definitions for utility availability without relevant simulation, the proposed framework in the current study explicitly simulates building-level utility service availability. Utility service availability is based on community-level network analysis, as described subsequently in this paper.

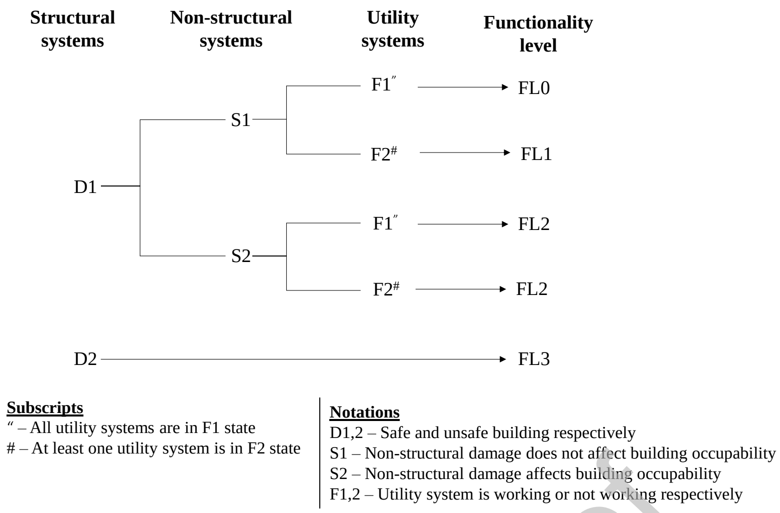

Figure 3 – Defining post-event functionality level using a fault tree

FL0 corresponds to a functionality level whereby a building is occupiable and safe with 100% functionality of all utility systems. An FL1 building is safe and occupiable, but there is reduced functionality due to a faulty utility system. An FL2 building is unoccupiable due to a damage state S2 for the nonstructural system. It is, however, noted that buildings in FL2 could be used as shelter-in-place. An FL3 building is an unsafe building with extensive or complete damage to the structural system.

3.4 Decision-making on intervention

Once the functionality level is determined, a decision is made on the appropriate intervention strategy. A decision-making flowchart is presented in Figure 4. The flowchart assumes that buildings in FL1 and FL0 are in a repairable state, and any minor damage to the systems will not compromise the response of the building in an aftershock. However, it is also assumed that repairs that are not safety-critical can be done while the building is in continued use. An

FL3 building requires partial or total replacement, and relocation may be necessary in some instances (e.g., buildings located in liquefiable soil).

A decision-making analysis is required to decide whether an FL2 building would be decommissioned or not. Such analysis could be done by comparing the mean loss ratio (i.e., the repair cost to the total replacement cost of the building) to a predetermined threshold (e.g., FEMA 2012), a cost-benefit analysis, or a multicriteria decision-making analysis. The choice of the analysis type is dependent on the decision-makers.

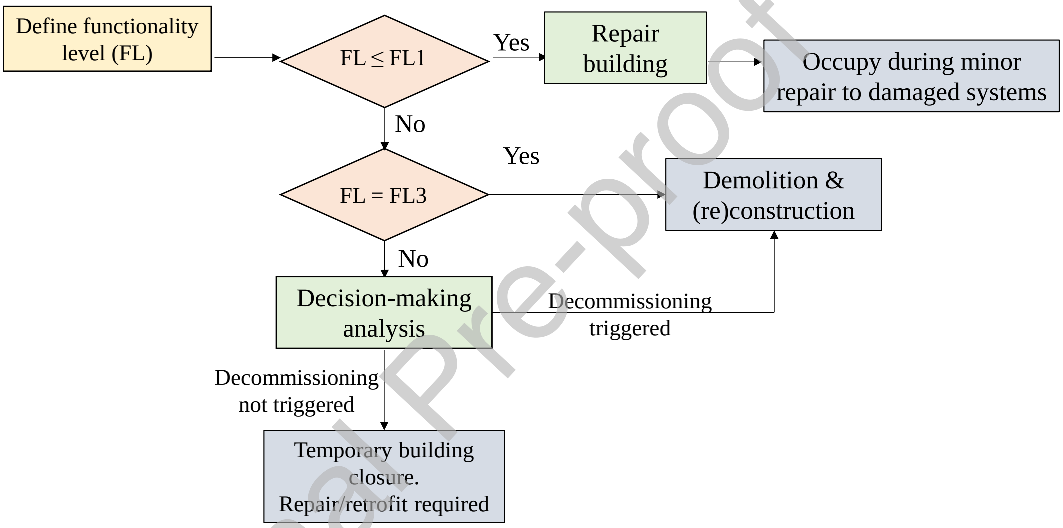

Figure 4 – Flowchart for decision-making on required intervention for each building

3.5 Intervention prioritization at the community-level

Community-level intervention requires substantial resources – including workforce, time, funding, and material. Appropriate resource allocation is essential to mitigate the adverse socioeconomic impacts of a prolonged recovery process. As highlighted in past studies (e.g., Peacock et al., 2014), fragmented and unequal intervention strategies significantly impact socially vulnerable communities. To achieve an inclusive recovery process in government (or any centrally)-managed intervention projects, it is crucial to adopt an intervention prioritization model incorporating all socioeconomic, political, and cultural factors. Key factors to consider include the political importance of buildings requiring intervention (political factor), social vulnerability indicators of people in affected buildings (socioeconomic), available budget for intervention (socioeconomic), land availability for relocation (socioeconomic and environmental), and the historical and cultural significance of the affected buildings (cultural). An intervention prioritization list for affected buildings can be developed using a multicriteria decision-making (MCDM) framework, which entails (a) developing criteria weights for each of the considered socioeconomic, cultural, and political factors using the analytical hierarchy process (Saaty 1980) for criteria weight calibration; (b) defining performance measures, corresponding to the considered factors, for each affected building; (c) combining the criteria weights and performance measures to develop the prioritization list using the technique for order of preference by similarity to ideal solution (TOPSIS) (Hwang and Yoon 1981) for the ranking process. The criteria weights are defined based on the importance level assigned to each criterion by the decision-makers. For the sake of brevity, detailed discussions on criteria weights calibration and ranking process in MCDM frameworks are omitted. Detailed discussions are available in Saaty (1980), Hwang and Yoon (1981), and Opabola and Galasso (2022). Other optimization algorithms, aside from the recommended AHP + TOPSIS, can be adopted if desired.

3.6 Recovery sequence for each building

The recovery sequence (including both the mobilization and intervention phases) for a building is selected based on the chosen intervention type. The average recovery time is assumed to be the sum of the average time required to inspect damaged buildings (T_{insp}), for the bidding and construction mobilization (T_{mob}), and to restore functionality through the selected intervention process (T_{int}).

As shown in

Table 2, each task in the intervention sequence is linked with a corresponding functionality level $Q(T_i)$ attained after task i is completed at a given time T_i. Furthermore, considering workers' allocation, each task's ideal duration (w) in a pre-disaster scenario is also defined. However, the relocation and (re)construction sequence may be region- or building-specific. For instance, local authorities may have policies to relax or toughen construction design and planning processes following a disaster. Therefore, it is recommended that the intervention sequence be defined based on the local context.

Table 2 – Intervention sequence for a recovery project

Task	Preceding task	Functionality level (Q(t))	Duration			
			Ideal (w)	Optimistic (a)	Most likely (m)	Pessimistic (b)
Mobilization phase						
A	Disaster	$Q(T_A) = Q(0)$	w_A	a_A	m_A	b_A
B	A	$Q(T_B)$	w_B	a_B	m_B	b_B
C	A	$Q(T_C)$	w_C	a_C	m_C	b_C
D	B	$Q(T_D)$	w_D	a_D	m_D	b_D
E	B,C	$Q(T_E)$	w_E	a_E	m_E	b_E
Intervention phase						
F	D,E	$Q(T_F)$	w_F	a_F	m_F	b_F
G	E	$Q(T_G)$	w_G	a_G	m_G	b_G
H	F	$Q(T_H)$	w_H	a_H	m_H	b_H
I	H,G	$Q(T_I)$	w_I	a_I	m_I	b_I
Target recovery		$Q(T_{target})$				

3.7 Recovery time modeling using stochastic network analysis

This study uses network analysis techniques to model buildings' recovery time. Network analysis is a project management approach that supports the planning of projects by identifying the interrelationships between tasks or activities making up complex processes. Network analysis can be used to determine the critical path for complex projects. The critical path indicates the required minimum timeframe to complete a given project. Network analysis techniques are either deterministic (e.g., Critical Path Method - CPM) or probabilistic (e.g.,, Program Evaluation and Review Technique – PERT; or Monte Carlo Sampling - MCS).

Deterministic network analysis techniques do not consider the time to complete a task as a random variable. To account for delays, time buffers are applied to each task. This approach adds flexibility to the recovery time evaluation process; however, a series of delay-inducing events can result in extended recovery time, which time buffers cannot adequately cover (Goldratt 1997). Stochastic network analysis techniques account for anticipated delays in each recovery task (and the uncertainties associated with these delays) in a probabilistic manner, such that the evaluated recovery time is probabilistic. PERT is most reliable when a project has only one path. However, typical projects have multiple paths, so MCS is typically the preferred analysis method. Hence, this study adopts MCS to evaluate the recovery time of buildings.

The recovery time R_t to attain a given functionality level *Q(t)* is defined as a function of the mobilization time M_t and the intervention time I_t and can be expressed as

$$R_t\,(Y) = f\,[M_t\,(Y),\, I_t\,(Y), Q(0), Q(t)], \tag{1}$$

where Y is a set of variables characterizing the selected intervention strategy for the building (i.e., repair, retrofit, replacement, or relocation), and *Q(0)* is the initial post-event functionality level.

Table 2 and Figure 5 depict the intervention sequence and a hypothetical network diagram of a recovery process (i.e., repair, retrofit, reconstruction, or relocation) disaster-damaged building. The tasks (A to I) are tasks within the building's emergency, transition, and recovery phases. Each task is characterized by a single task duration in a deterministic analysis using CPM. However, when employing MCS, each task is characterized by three durations – the optimistic duration (*a*), the most likely duration (*m*), and the pessimistic duration (*b*). The three duration parameters for each task are defined from the average time (*w*) to complete a task in an ideal (typically pre-disaster) scenario using recovery time amplification and mitigation factors. The defined duration parameters (i.e., *a*, *m*, and *b*) are then used to generate a PERT distribution for each task duration (e.g., (Clark 1962; Hajdu 2013; Keefer and Verdini 1993). The defined probabilistic duration parameters for each task are then used to carry out MCS (Burt and Garman 1971; Van Slyke 1963). This entails conducting critical path analyses (for a chosen number of iterations) using randomly chosen task durations in each iteration (i.e., equal likelihood of selecting *a*, *b*, or *m*). The expected critical path and critical path duration (i.e., expected recovery time) are evaluated for each iteration. Once the iterations are completed, it is then possible to evaluate the recovery time distribution required to attain the functionality level after each intervention task is completed – the analysis output.

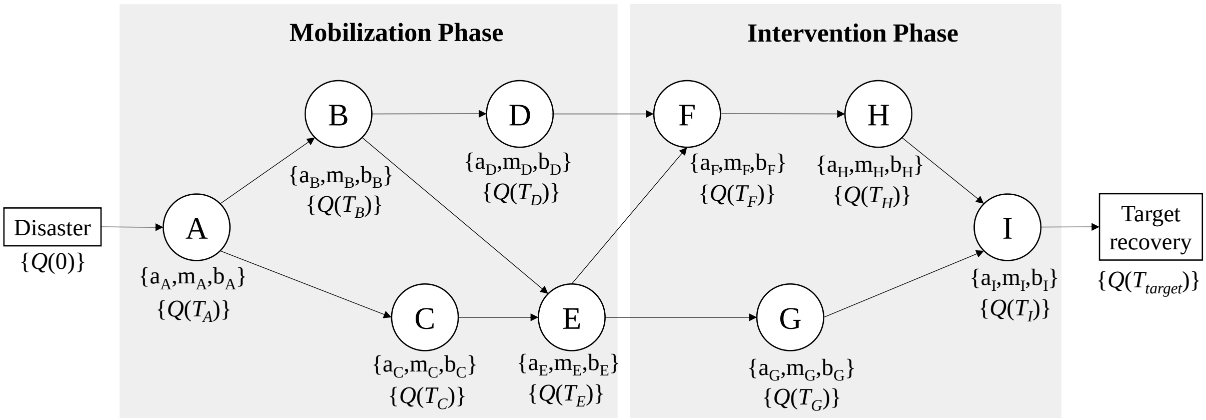

Figure 5 – Hypothetical network diagram for the recovery process of a building

In this study, amplification and mitigation factors account for socioeconomic, political, environmental, and cultural conditions expected in a disaster-hit community. These factors explicitly account for the availability of human and material resources, inflation, land-related issues, environmental conditions, availability of transportation channels, political environment, security-related issues, bureaucracy, design and construction practice, finance-related matters (e.g., delay in sourcing for donors and foreign aids), epidemic-related issues, socio-cultural issues, and level of community participation.

Amplification and mitigation factors are either time-dependent or not. If a factor is deemed to be time-dependent, a time-series function needs to be defined. Figure 6 illustrates two types of time-series functions for the factors – reversing and non-reversing. A reversing time-series function is relevant in a case where the amplification or mitigation factor increases and decreases intermittently over time (Figure 6a). Examples of cases where reversing factors may be required include government-imposed intermittent lockdowns (during a pandemic) and weather conditions affecting site productivity. A non-reversing time-series function is relevant when the amplification or mitigation factor increases or decreases to a peak value and balances off (Figure 6b). An example of cases where non-reversing factors may be applied includes the influence of material cost increase on recovery time and cost. Studies (e.g., Chang et al. (2011)) provide data on material costs versus time following the 2008 Wenchuan earthquake. Reversing and non-reversing factors can be modeled using a wave function fitted to available data. Another approach is to model a non-reversing factor by defining four time parameters (Figure 6b) – 1) the time when amplification/mitigation starts (t_1); 2) the time when amplification or mitigation factor reaches its peak (t_a); 3) the time when amplification or mitigation factor starts deteriorating (t_b); and 4) the time when no amplification/mitigation occurs (i.e., returns to pre-disaster scenario) (t_c). A reversing factor can also be modeled by defining t_1, t_a, t_b, t_c for each half-cycle.

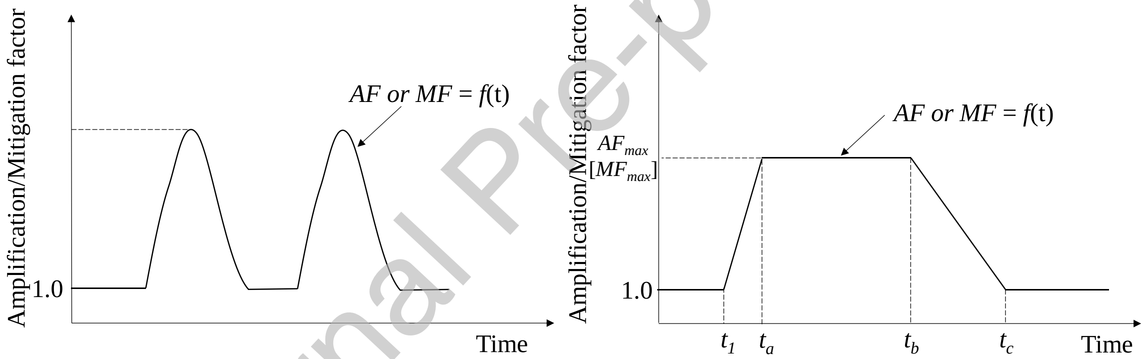

(a) Reversing factor (b) Non-reversing factor

Figure 6 – Time-dependent factors

The recommended amplification and mitigation time overrun multipliers are provided in Table 1. No recommendations are provided on the time parameters for time-dependent factors because such parameters would significantly vary from region to region. It is recommended that these parameters are defined based on relevant local context. However, typical peak values for time-dependent factors are provided in Table 1. It is also noted that the list provided in Table 1 is not exhaustive or definite. Users can use knowledge of the socioeconomic, cultural and political setting of their case study region to select the appropriate factor when adopting Table 1.

Once the amplification and mitigation factors for each task in the intervention sequence are defined, the optimistic duration (*a*), the most likely duration (*m*), and the pessimistic duration (*b*) can be computed. The optimistic duration (*a*) is the minimum time to complete a task in the recovery process, assuming all the expected time mitigation factors are activated and there are no time-amplification factors. The optimistic duration (*a*) for task *i* can be estimated using Equation (2).

$$a_i(t) = \prod_{l=1}^{p} MF_{li}(t) \times w_i \qquad (2)a$$

$$a_i(t) = \max\left\{MF_{li}(t)\right\} \times w_i \qquad (2)b$$

Equations (2)a & b are recommended when the mitigation factors are assumed to have sequential and concurrent impacts, respectively. In Equation (2), *w* is the average time to complete a task in an ideal pre-disaster situation, *l* is the number of mitigation factors (MF) (*l* = 1, 2.., *p*) influencing task *i*. A value of MF is selected from Table 2. As previously mentioned, mitigation factors may be time-dependent, which must be accounted for when calculating *a*.

The pessimistic duration (*b*) is the maximum time to complete a task assuming all the time amplification factors are activated and there are no time mitigation factors. The pessimistic duration (*b*) can be estimated using Equation (3). Equations (3)a & b are recommended when the amplification factors are assumed to have sequential and concurrent impacts, respectively.

$$b_i(t) = \prod_{n=1}^{q} AF_{ni}(t) \times w_i \qquad (3)a$$

$$b_i(t) = \min\left\{AF_{ni}(t)\right\} \times w_i \tag{3)b$$

The most likely duration (*m*) captures the highest likelihood of completing the task in a given timeframe. *m* is defined to be closer to *a* if there is a higher likelihood that the mitigation factors would be more prevalent than the amplification factor or closer to *b* otherwise. When uncertain, *m* can be defined as 0.5(*a*+*b*).

4 MODELING ELECTRIC POWER DISRUPTION

4.1 Defining fragility functions for EPN components

EPNs comprise three main systems – generation, transmission, and distribution. The generation system is mainly made up of power-generating plants. The transmission system includes electrical substations (including primary components such as transformers, breakers, and switches), transmission towers, and lines. Finally, the distribution system consists of distribution poles, distribution conductors, pole-mounted transformers, and service drops.

Fragility models for power systems are typically in the form of binary states (i.e., fail or survive) or in the form of continuous fragility functions for multiple damage states (as a function of a hazard IM). Several studies (e.g., Ang et al. 1996; FEMA 2003; Shinozuka et al. 2007; Straub and Der Kiureghian 2008; Vanzi 2000) have developed numerical and empirical fragility models for generation, transmission, and distribution systems under various hazard demands at the system and component levels. Dueñas-Osorio et al. (2007) have also developed fragility models for an entire power grid. A detailed review of all available fragility functions is outside the scope of this paper.

If a system-level fragility function is available, it can be adopted in the proposed framework (Figure 2). On the other hand, if only component-level fragility functions are available, the probability of a system being in a functionality level, given the functionality states of its components at a given hazard intensity level, can be computed as

$$P\left(S_j = s \middle| IM\right) = P\left(S_j = s \middle| \bigcap_{i=1}^{n_j} C_i = c_i\right) P\left(\bigcap_{i=1}^{n_j} C_i = c_i \middle| IM_i\right), \tag{4}$$

where *s* is the functionality level of system *j* (equals 0 for a functioning system and 1 for a nonfunctioning system), C_i is the functionality level of component *i* (equals 1 if component *i* suffers at least a moderate damage or 0 otherwise); $P\left(S_j = FL \middle| \bigcap_{i=1}^{n_j} C_i = c_i\right)$ is the conditional probability of a system *j* having a functionality level FL given the events of its components; $P\left(\bigcap_{i=1}^{n_j} C_i = c_i \middle| IM_i\right)$ is the conditional probability of a component being functional given a hazard intensity measure (IM) at the site of component *i*.

4.2 Initial operability assessment framework

As shown in Figure 2, an operability assessment is carried out after the fragility functions for all the systems and components have been defined. The flowchart for the operability assessment is presented in Figure 7. The flowchart builds on lifeline loss estimation modeling frameworks described in past studies (e.g., Chang et al. 2002; Mensah and Dueñas-Osorio 2016) for wind-related hazards. Firstly, the region of interest is divided into service areas. Each service area is supplied by one substation. Next, an adjacency matrix for the distribution network is assembled. This shows the connections between the substation supplying the service area and the distribution load points (i.e., Figure 9b) within the service. Once the adjacency matrix is developed, given the hazard intensity level (simulated through MCS at each location of interest) and fragility functions, *N* realizations of component and system functionality states are defined. For each realization, the number of consumers served is estimated, as shown in Figure 7. The initial post-event operability of the power system $Q_p(0)$ is then taken as the ratio of the number of consumers served immediately after the disaster to the number of consumers served pre-disaster. If the state of a generation system is simulated as nonfunctional, a total power shutdown is assumed (i.e., $Q_p(0) = 0$). Otherwise, the functionality of each substation is assessed. The consumers within a service area with a nonfunctioning substation are assumed to have lost power access. For functioning substations, the adjacency matrix is updated based on the simulated functional state of the components in the distribution network. A path-finding algorithm is then used to evaluate the presence of a distribution link between the consumer and the substation. All consumers without a functional link with a functioning substation are assumed to have lost power access.

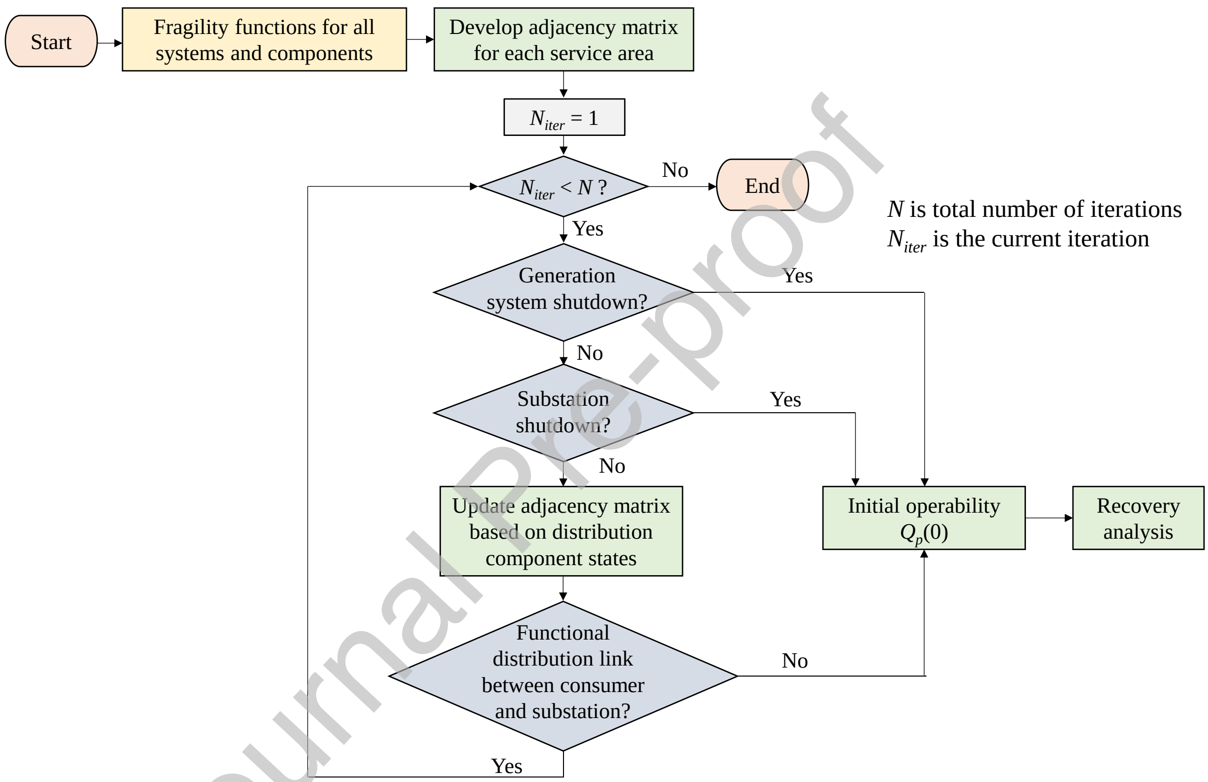

Figure 7 – Initial operability assessment framework for an electric power network

The output of the initial operability assessment framework is the probabilistic distribution of the initial post-event operability $Q_p(0)$, given the N realizations of components and system functionality states (corresponding to the simulated N IM realizations at each considered site). For each realization, the recovery time can be estimated using simulation techniques as the time to repair or replace damaged components and systems (e.g., Çağnan et al. 2006).

However, similar to the discussions previously presented for structural systems, several complexities are associated with estimating the downtime of power systems. For example, one must assume a restoration sequence and concurrency for the damaged components. The number of possible sequences would be 2^{ns} (where *ns* is the number of damaged components needing restoration). Aside from that, the influence of various factors on the downtime of each component would need to be accounted for. Hence, the current study proposes a different, simplified approach for estimating downtime as a function of initial post-event operability.

4.2.1 Recovery time modeling

A literature survey was conducted to identify studies where the initial post-disaster operability (i.e., in terms of the number of people served or the number of operating power stations) and downtime have been reported. Recovery time is defined as the time to restore the functionality to 100%. The focus of the literature survey was developing countries. Key references where relevant information has been provided are Didier et al. (2017), Dueñas-Osorio and Kwasinski (2012), and Miyamjima et al. (2018). Notably, most available literature on the recovery of power systems does not provide information on the initial post-disaster operability. For example, Ahmadizadeh and Shakib (2004) only reported four-day downtime for a substation following the 2003 Bam earthquake without any information to quantify the post-disaster operability in the region.

Figure 8 presents the available data reported on the initial post-disaster operability and recovery time for disaster-hit regions following the 2010 M_w 8.8 Maule Earthquake (Dueñas-Osorio and Kwasinski 2012), 2017 Mw 7.3 Iran-Iraq Earthquake (Miyamjima et al. 2018), and 2015 M_w 7.8 Gorkha Earthquake (Didier et al. 2017). Dueñas-Osorio and Kwasinski (2012) provide multiple data points on the recovery pathway and time for two cities and a region. As shown in Figure 8, the recovery time for the power system R_{pT} is highly correlated to the initial post-event operability. The relationship between recovery time and initial post-event operability can be taken as

$$R_{pT} = 180e^{-10Q_p(0)}, \text{ in days} \tag{5}$$

Equation (5) provides an R^2 of 0.95. It is noted that the current data is limited. Hence, additional data are needed to validate Equation (5). For probabilistic modeling purposes, by fitting a logarithmic CDF to the error of Equation (5), it was determined that a logarithmic dispersion of 0.7 be used to simulate modeling uncertainty for Equation (5).

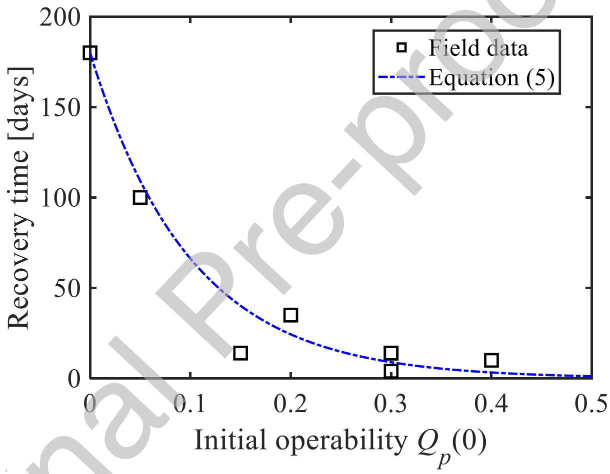

Figure 8 – Recovery time for power systems as a function of the initial post-event operability

Given that Equation (5) is empirical, it inherently accounts for some degree of local factors (e.g., availability of technical and human resources) that influence the overall recovery time. However, if deemed warranted by decision-makers, the calculated recovery time can be modified by using amplification factors similar to those in Table 1.

4.3 Recovery trajectory of electric power networks

It might seem reasonable to model the recovery trajectory for EPN based on the optimal intervention sequence (i.e., repair sequence of damaged transmission and distribution systems). However, socioeconomic and political factors can highly influence such a trajectory. For example, a government may decide to focus interventions on affluent residential areas rather than follow an optimal sequence. Also, political conflict may influence the intervention sequence.

This study recommends two approaches that may be adopted for modeling the recovery trajectory of EPNs. The first entails defining intervention sequences for the entire network and restoration time for each damaged component (e.g., Shinozuka et al. (2004)). The second approach involves defining a recovery trajectory function based on the expected level of preparedness, technical know-how, and impeding conditions (i.e., socioeconomic and political). Cimellaro et al. (2010) recommend trigonometric and exponential functions for poorly- and well-prepared communities, respectively. Cimellaro et al. (2010) recommend a linear function for cases without the knowledge of preparedness, resource availability, and societal response. Rather than adopting separate functions, this study proposes a unified recovery trajectory function for EPNs (Equation (6)). The functionality level Q at a given t can be taken as

$$Q(t) = Q(0) + \frac{g\left(\frac{t - t_m}{R_t - t_m}\right)}{1 + gh\left(\frac{t - t_m}{R_t - t_m}\right)}, \tag{6}$$

where g and h are shape constants that quantify the recovery rate of the system, t_m is the mobilization time, R_t is the recovery time computed using Equations (5) and (6) for power and water networks, respectively.

The values of g and h express the level of preparedness, resource availability, and societal conditions of a community. For any value of h, g can be computed as:

$$g = \frac{Q(R_t) - Q(0)}{Q(0)h - h + 1}, \tag{7}$$

where $Q(R_t)$ is the functionality level once the recovery time is attained. For complete recovery, $Q(R_t)$ equals unity. $Q(R_t)$ can be greater than unity if the target functionality level is higher than the pre-event functionality level (e.g., in a build-back-better scenario).

Depending on the value of h, the recovery curve derived using Equation (6) could either be concave, convex, or linear. Figure 9 depicts three different recovery trajectories for a power network with initial post-event operability of 0.25 and a recovery time of 50 days, assuming $h = -10$, $h = 1.5$, and $h = 0$. A concave recovery curve corresponds to $h << 0$ and represents the recovery trajectory of a community with a poor level of preparedness, a high level of resource unavailability, and unfavorable societal conditions. In contrast, $h >> 0$ represents a community with a good level of preparedness, good resource availability, and unfavorable societal conditions. h can be estimated by curve fitting to the available historical data on the recovery trajectory. As an alternative, recovery rate models calibrated to past events can also be used in estimating the value of h. Several studies (Barabadi et al. 2011; Barabadi and Ayele 2018; Gao et al. 2010) have developed regression models for predicting the recovery rate of utility networks. For example, Barabadi and Ayele (2018) proposed an empirical formulation for predicting the recovery rate of electric power networks as a function of hazard type, age and condition of power systems, time of the event, post-event operability, and length of the distribution feeders.

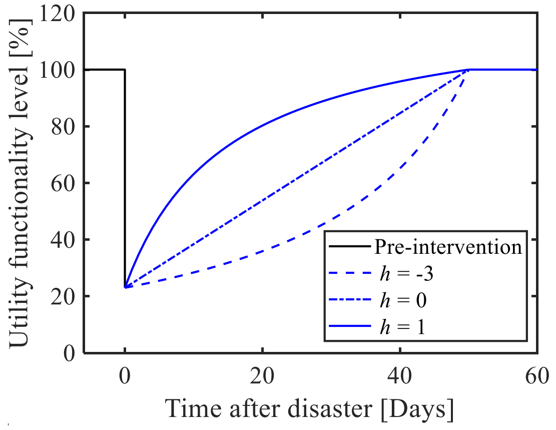

Figure 9 – Recovery trajectories for a community considering various levels of impending conditions

5 CASE STUDY

5.1 Overview

The proposed framework is illustrated through four case studies to model the post-earthquake recovery of a synthetic small-scale residential community with a population of 22,500 people (Figure 10). Synthetic testbeds have gained widespread use in disaster risk management, particularly to test, verify, and validate community resilience models/tools (e.g., Amin Enderami et al. 2022). Each case study intends to demonstrate how local authorities can adopt the proposed framework as a disaster risk management tool for specific objectives.

The synthetic residential community consists of a building stock of 450 reinforced concrete (RC) frame buildings comprising 150 two- and 300 four-story frames with an average occupancy of 10 households per building. It is assumed that the two-story buildings are low-cost housing with lower floor space per occupant compared to the four-story buildings. Each household is assumed to consist of five members, making a total of 22,500 occupants in the hypothetical residential community. Most buildings in the residential community (90%) are assumed not designed to modern seismic codes and are susceptible to non-ductile behavior. The remaining 10% of the building stock is code-conforming.

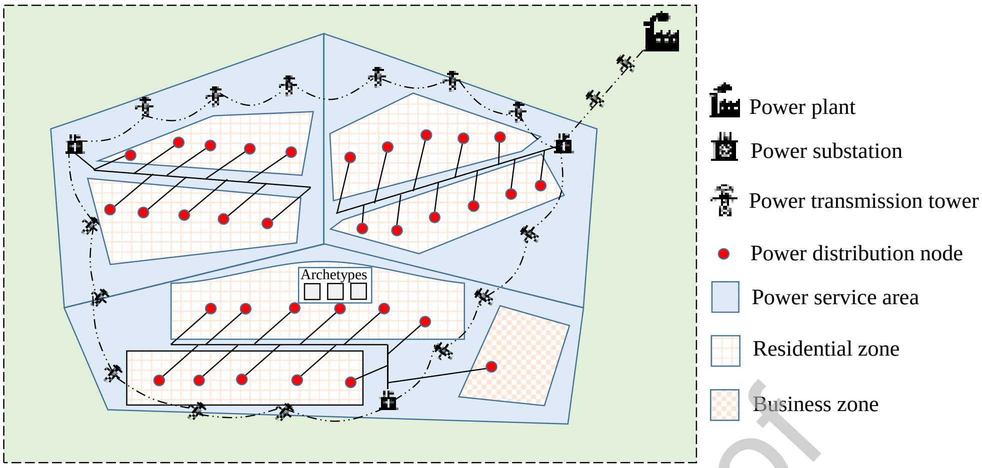

Figure 10 – Case study community

It is assumed that the community is supplied by three power substations (Figure 10). Each service area (for each substation) is assumed to supply 150 buildings, corresponding to 1,500 households and 7,500 consumers. For the sake of simplicity, a similar distribution system (i.e., links between substation and distribution nodes) is assumed for each service area.

5.2 Hazard analysis

The recovery modeling of the community is carried out for a moment magnitude 7 scenario occurring from a normal fault situated about 20km from the community. A V_{s30} of 360m/s is assumed for the community as a whole. The hazard analysis uses the Campbell and Bozorgnia (2014) ground-motion model to derive spectral accelerations at the building locations, substation sites, and distribution nodes. Furthermore, the Markhvida et al. (2018) approach is used to generate 1,000 realizations of spatially cross-correlated spectral intensities at the building locations, substation sites, and distribution nodes, using Principal Component Analysis.

It is noted that, due to the limited availability of recorded ground motions in developing countries, regional ground motion models may be unavailable or unsuitable for developing cross-correlated IMs. Scoring criteria can be used to select the best models for specific applications (e.g., Stewart et al., 2015). Another alternative is to perform physics-based ground motions simulations (e.g., Jenkins et al., 2023). However, this study has not followed this approach given the illustrative nature of the case-study application relying on a synthetic testbed.

5.3 Case study 1: Capturing the impact of improving EPN

This case study demonstrates how the proposed methodology can capture the impact of various strategies for improving the EPN. Four scenarios are considered – scenario 1-1 is the current state with no improvement. Scenario 1-2 entails providing seismic anchors for components of the substations, Scenario 1-3 entails retrofitting the distribution circuits (without providing seismic anchors for components of the substations), and Scenario 1-4 combines scenarios 1-2 and 1-3.

The fragility functions for the substation and distribution circuits are derived from FEMA (2022). For each of the thousand realizations of spatially correlated peak ground accelerations, the functional states of substation and distribution nodes are used in assessing the number of consumers without access to the power network in the community. The initial post-event operability for each simulation is defined as the number of consumers without access to power supply divided by 22,500 (i.e., 7,500 consumers per service area times three service areas) pre-earthquake consumers. The median recovery time for the calculated initial post-event operability is then calculated using Equation (5). Subsequently, the model uncertainty in Equation (5) is also propagated through MCS by sampling 1,000 realizations of each computed median recovery time using the recommended dispersion value for Equation (5). Figure 11 presents the output of the EPN analysis for each considered scenario.

The figure shows that each considered mitigation strategy (i.e., scenarios 2, 3, and 4) significantly reduced the median community-level power downtime. Retrofitting the substations and distribution circuits reduces the downtime from 24 to 4 days.

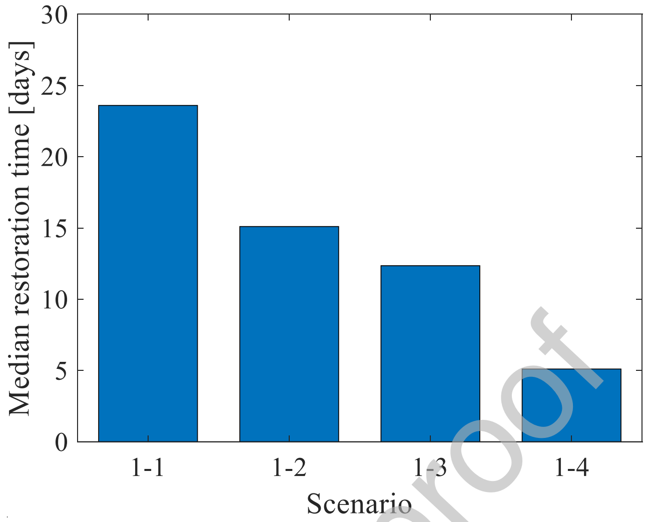

Figure 11 – Recovery time for the EPN for the four considered scenarios

Figure 11 can be helpful for analysts and decision-makers seeking to understand the effect of various EPN failure mitigation policies. Also, the recovery time estimates can inform homeowners and EPN companies on necessary measures (i.e., backup power sources and power disruption insurance) to counterbalance potential hazards in their communities. Although not demonstrated here, the recovery modeling framework can be combined with a cost analysis for decision-makers to better inderstand the cost-benefit ratios of each mitigation policy.

5.4 Case study 2: Impact of socioeconomic factors on long-term community-level recovery

This case study demonstrates how the proposed methodology can capture the influence of socioeconomic factors on long-term community-level recovery, specifically rehousing of displaced people. Three scenarios are considered – scenario 2-1 is an ideal scenario with no recovery-impeding factors on reconstruction projects. Scenario 2-2 simulates a scenario where community conflicts and bureaucratic delays influence post-disaster reconstruction; scenario 2-3 represents a scenario with material procurement, construction worker skills, and funds issues. A similar workforce (i.e., 80 crews) is assumed for all scenarios. As shown in Figure 11, the EPN is restored in 24 days. Hence, the impact of the EPN outage on long-term recovery is negligible.

The probable functionality level of each building is estimated by combining the fragility functions for the structural and nonstructural systems with the IMs (spectral acceleration at 1s) at the building site. The seismic fragility models of the structural systems and nonstructural components are based on Villar-Vega et al. (2017) and FEMA (2022), respectively. For each of the thousand realizations of spatially correlated spectral accelerations that were simulated (note that these realizations were done collectively with the IM for the EPN analysis, i.e., peak ground accelerations), the post-event functionality level of each building is evaluated as described in the methodology section.

Given that the case study looks at long-term recovery, the recovery analysis focuses on reconstructing buildings recommended for reconstruction (See Figure 4). The calculation assumes that all displaced households are waiting (in temporary shelters) for the buildings to be rebuilt. A key assumption in this analysis is that no life was lost during the disaster, and each displaced household is provided with a new one-story single-family residential house.

The intervention sequence of the reconstruction process entails sourcing for reconstruction funds, planning, and building design, securing relevant permits, tender process and contracting engineers and builders, site clearing, site mobilization, and construction. The average time to complete each task in an ideal pre-disaster situation (w), adopted in Equations (2) and (3), for the reconstruction projects are based on information derived from actual construction projects of one-story single-family residential houses in Palu, Indonesia

(Opabola et al. 2023). The time amplification factors considered for each task and each scenario (to estimate the pessimistic time *b*) are based on the maximum of the range presented in Table 1. A unity factor is used to estimate the optimistic time (*a*). The most likely time is assumed to be 0.5(*a*+*b*).

Figure 12 compares the recovery curves of the three considered scenarios. As shown in the figure, accounting for socioeconomic factors significantly increases the time required for several families to return to permanent housing. According to the case study, community conflicts and bureaucratic delays increased community-level recovery time to more than five years (twice the period required in scenario 2-1).

Decision-makers could use such information to develop appropriate mechanisms to ensure full recovery in communities susceptible to communal conflicts, especially in cases where post-disaster conditions could escalate such conflicts.

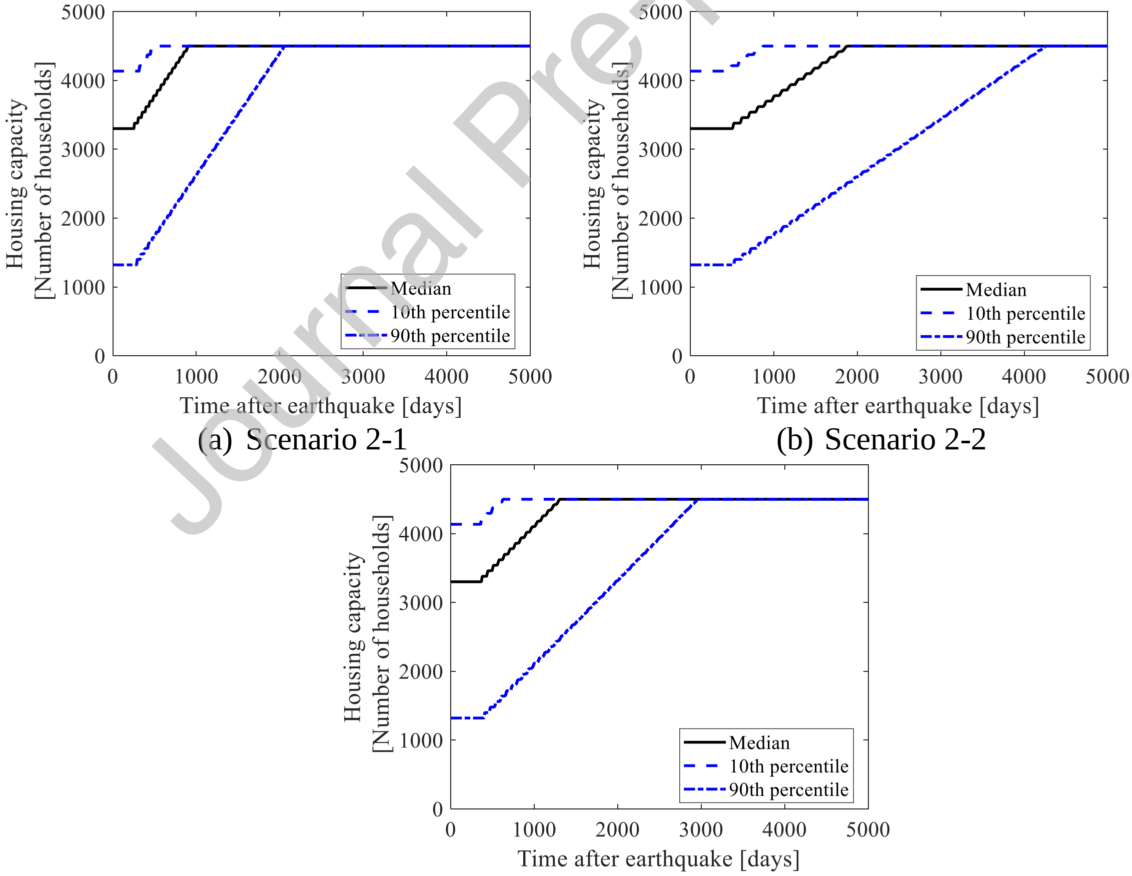

(a) Scenario 2-1

(b) Scenario 2-2

(c) Scenario 2-3

Figure 12 – Community-level housing capacity recovery for (a) Scenarios 2-1; (b) 2-2; and (c) 2-3.

Delays associated with material procurement, construction worker skills, and funds issues (scenario 2-3) could result in less downtime than scenario 2-2. This is attributed to the fact that funds issues may be present during the initial phases of the project (the case assumed in the analysis). However, if funds-related issues are prevalent in each phase of the recovery project, the time to achieve full recovery may be prolonged.

5.5 Case study 3: Impact of increased expert workforce on long-term community-level recovery

This case study demonstrates how the proposed methodology can capture the influence of increasing the expert workforce in a community on long-term post-disaster recovery. Two scenarios are considered – scenario 3-1, which assumes only 80 crews of construction workers, and scenario 3-2, with 160 crews of construction workers.

The post-disaster functionality level and housing capacity are estimated similarly to the preceding case study. A similar reconstruction sequence is also adopted. However, the number of construction crews is varied to capture the scenarios of interest. Regarding recovery-impeding factors, only delays due to material procurement are considered. The influence of other socioeconomic and political factors is also ignored. It is also assumed that the workforce is well-trained. Hence, no delays due to poor management skills are considered.

Figure 13 compares the community-level housing capacity recovery curves for the two scenarios. As shown in the figure, doubling the workforce reduces the median recovery time by 60%. Local authorities can use such information to plan the number of crews that must be sourced locally and/or otherwise to meet a target recovery time.

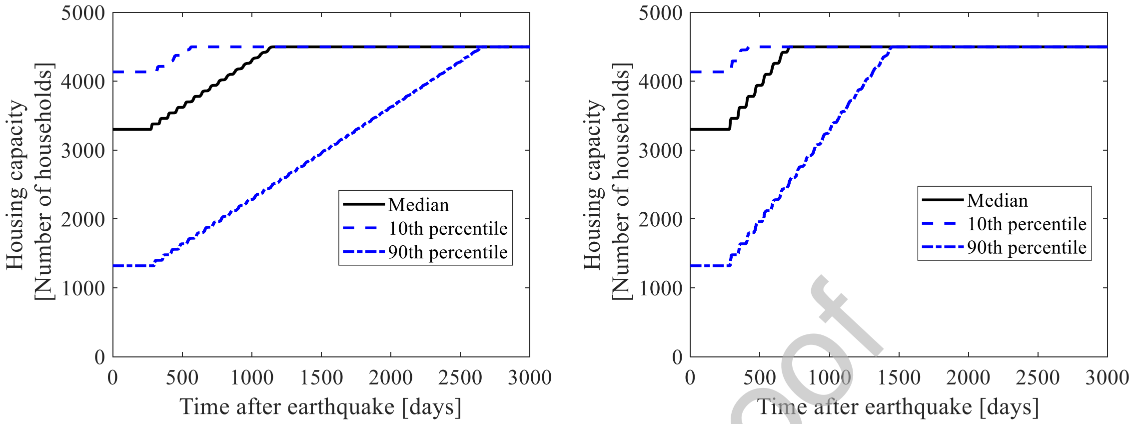

(a) 80 construction crews (b) 160 construction crews

Figure 13 – Community-level housing capacity recovery for case study 3 considering (a) 80 construction crews (scenario 3-1); (b) 160 construction crews (scenario 3-2)

5.6 Case study 4: Impact of structural retrofit policies on long-term community-level recovery

This case study demonstrates how the proposed methodology can capture the influence of retrofit policies on community resilience. This study assumed a similar social vulnerability index for the entire community. Hence, the selection of low-code buildings for retrofit is based mainly on distance from the fault (i.e., low-code buildings closer to the fault are considered for retrofit). This assumption is adopted because the same fragility functions were adopted for the buildings (but different sets of fragility functions for different building heights). The fragility functions for the retrofitted buildings are based on Opabola et al. (2021).

Four scenarios are considered. Scenario 4-1 assumes no retrofit (i.e., 90% of the entire building stock remains non-ductile). Scenario 4-2 considers retrofit of 25% of the total low-code buildings closest to the fault (irrespective of the number of stories) – a total of 101 buildings are retrofitted. Scenario 4-3 considers retrofit of 50% of total low-code buildings closest to the fault (a total of 202 buildings are retrofitted). Scenario 4-4 assumes retrofit of 75% of the total low-code buildings closest to the fault. Finally, scenario 4-5 considers retrofit of all low-code buildings.

Regarding recovery-impeding factors, only delays due to material procurement are considered. A similar workforce (i.e., 80 construction crews) is assumed for all scenarios. Figure 14 compares the normalized median post-earthquake housing capacity (defined as the ratio of the number of households with access to a permanent residence to the total number of households), the median time to achieve full community recovery (i.e., construct all new permanent houses), and the proportion of retrofitted low-code buildings. For example, as shown in the figure, retrofitting 50% of the low-code buildings increases the normalized median post-earthquake housing capacity to 90% (from 70%) and reduces the median full recovery time by 40%.

Case study 4 is relevant in cases where local authorities want to identify buildings that need to be prioritized for retrofit based on the fact that retrofitting such buildings significantly enhances community-level recovery.

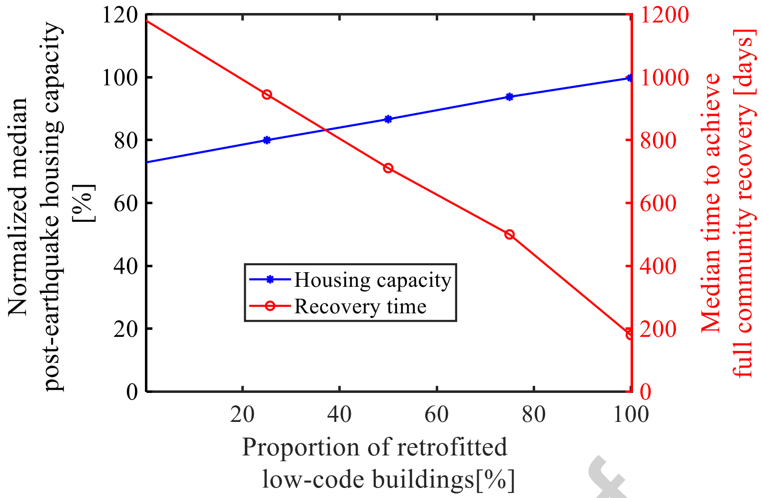

Figure 14 – Relationship between normalized median post-earthquake housing capacity (defined as the ratio of the number of households with access to a permanent residence to the total number of households), the median time to achieve full community recovery (i.e., construct all new permanent houses), and the proportion of retrofitted low-code buildings

Figure 15 combines the output of case studies 1 and 4 to demonstrate how local authorities could identify the proportion of households in the community with access to buildings that can achieve immediate post-event functional recovery (i.e., FL0 and FL1 buildings). As shown in Figure 15, building retrofit policies must be closely associated with EPN retrofit policies to ensure that a significant proportion of households do not need to suffer downtime from building or utility network damage. The proportion of households with access to a FL0 or FL1 building increases by 2.5 times when both the transmission and distribution systems of the EPN are retrofitted. It is also noted that a significant proportion of buildings in scenario 4-5 were classified as FL2 mainly because of power outage. While Figure 11 estimates a median recovery time of about 5 days for EPN in scenario 1-4, the importance of building-level power backup system can help ensure retrofitted buildings achieve immediate post-event functional recovery.

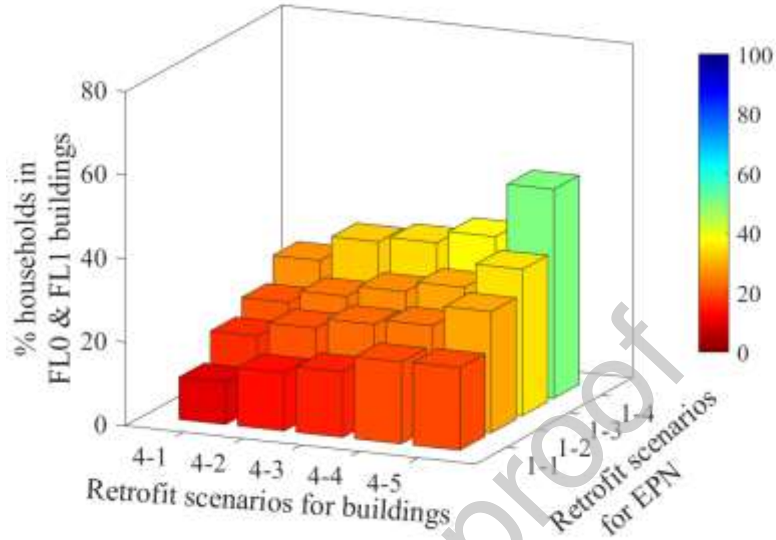

Figure 15 – Influence of retrofit scenarios for buildings and EPN on immediate functional recovery of buildings

Although not demonstrated here, Figure 15 can be combined with a cost analysis for decision-makers to better understand the cost-benefit implications of each mitigation policy. The analysis presented in Figure 15 is relevant in cases where decision-makers want to quantify the proportion of households that will have post-disaster liveable conditions (i.e., safe and occupiable buildings with access to electricity) following an event. Such data can be helpful in developing efficient post-event management strategies.

6 CONCLUSIONS

Local authorities and decision-makers need to access efficient and reliable disaster planning and management tools to achieve desirable levels of community resilience. This study proposes a probabilistic framework for modeling the post-disaster recovery pathway of a community's functionality blocks (i.e., buildings, electric power networks) at the community- and building levels. The novel aspects of the proposed framework include (a) introducing a multicriteria decision-making approach for community-level intervention sequencing, while capturing the influence of technical, socioeconomic, political, environmental, and cultural factors; (b) developing a stochastic network analysis approach for estimating the recovery time of damaged buildings, using proposed recovery time amplification and mitigation factors which are dependent on technical, socioeconomic, political, environmental, and cultural conditions of a community; (c) developing empirical formulations (based on historical data) to predict the community-level recovery time of power networks as a function of initial post-disaster outage level; and (d) the development of an approach for simulating historical recovery trajectory scenario on electric power networks. The output of the proposed framework is the probabilistic distribution of recovery times and various resilience indicators (e.g., the proportion of homeless households, the proportion of the population with access to power supply).

The proposed framework is demonstrated using a hypothetical community subjected to an earthquake scenario. The case study is used to assess the probabilistic recovery pathway of the EPN in the community and demonstrate how various mitigation strategies can influence the recovery time of the EPN. Furthermore, the case study captures the influence of various technical, environmental, socioeconomic, political, and cultural factors on post-disaster housing reconstruction. The analysis shows that, due to negative socioeconomic, political, and cultural factors, internally displaced people might remain homeless for up to five years after the disaster. The analysis also shows how community-level building retrofit policies can be designed by accounting for the quantified benefits of the retrofit to improve community resilience.

Based on the outcome of the case study, it is recommended that local authorities invest in policies that ensure the considered factors (i.e., consider the influence of conflicts within the community, bureaucratic delays, lack of community participation, and poor onsite construction management) are mitigated.

7 ACKNOWLEDGEMENTS

The study was carried out through the MultiVERSE project, funded by the UK Research and Innovation (UKRI) with project reference EP/X023710/1.

8 REFERENCES

ADB. (2007). *Proposed Loan for the Reconstruction of the Cement Production Facility in Aceh*. Jakarta.

ADB. (2009). *Earthquake and Tsunami Emergency Support Project (ETESP) – Indonesia*.

Aghababaei, M., and Koliou, M. (2022). “Community resilience assessment via agent-based modeling approach.” *Computer-Aided Civil and Infrastructure Engineering*.

Aghababaei, M., Koliou, M., Pilkington, S., Mahmoud, H., van de Lindt, J. W., Curtis, A., Smith, S., Ajayakumar, J., and Watson, M. (2020). “Validation of Time-Dependent Repair Recovery of the Building Stock Following the 2011 Joplin Tornado.” *Natural Hazards Review*, 21(4).

Ahmadizadeh, M., and Shakib, H. (2004). “On the December 26, 2003, southeastern Iran earthquake in Bam region.” *Engineering Structures*, 26(8), 1055–1070.

AIR. (2021). *Demand Surge Perspective on European Extratropical Cyclones*. Boston, MA.

Almoghathawi, Y., Selim, S., and Barker, K. (2023). “Community structure recovery optimization for partial disruption, functionality, and restoration in interdependent networks.” *Reliability Engineering & System Safety*, 229, 108853.

Almufti, I., and Willford, M. (2013). “The resilience-based earthquake design initiative (REDi^{TM}) rating system.” (October), 1–133.

Amin Enderami, S., Mazumder, R. K., Dumler, M., and Sutley, E. J. (2022). “Virtual Testbeds for Community Resilience Analysis: State-of-the-Art Review, Consensus Study, and Recommendations.” *Natural Hazards Review*, 23(4).

Ang, A.-S., Pires, J. A., and Villaverde, R. (1996). “A model for the seismic reliability assessment of electric power transmission systems.” *Reliability Engineering & System Safety*, Elsevier, 51(1), 7–22.

Barabadi, A., and Ayele, Y. Z. (2018). “Post-disaster infrastructure recovery: Prediction of recovery rate using historical data.” *Reliability Engineering & System Safety*, 169, 209–223.

Barabadi, A., Barabady, J., and Markeset, T. (2011). “Maintainability analysis considering time-dependent and time-independent covariates.” *Reliability Engineering & System Safety*, 96(1), 210–217.

Burt, J., and Garman, M. (1971). “Monte Carlo Techniques for Stochastic Pert Network Analysis.” *INFOR: Information Systems and Operational Research*, 9(3), 248–262.

Burton, H. V., Deierlein, G., Lallemant, D., and Singh, Y. (2017). “Measuring the impact of enhanced building performance on the seismic resilience of a residential community.” *Earthquake Spectra*, 33(4), 1347–1367.

Çağnan, Z., Davidson, R. A., and Guikema, S. D. (2006). "Post-Earthquake Restoration Planning for Los Angeles Electric Power." *Earthquake Spectra*, 22(3), 589–608.

Campbell, K. W., and Bozorgnia, Y. (2014). "NGA-West2 ground motion model for the average horizontal components of PGA, PGV, and 5% damped linear acceleration response spectra." *Earthquake Spectra*, SAGE Publications Sage UK: London, England, 30(3), 1087–1115.

Chang, S. E., and Shinozuka, M. (2004). "Measuring improvements in the disaster resilience of communities." *Earthquake Spectra*, 20(3), 739–755.

Chang, S. E., Svekla, W. D., and Shinozuka, M. (2002). "Linking infrastructure and urban economy: Simulation of water-disruption impacts in earthquakes." *Environment and Planning B: Planning and Design*, 29(2), 281–301.

Chang, Y., Wilkinson, S., Brunsdon, D., Seville, E., and Potangaroa, R. (2011). "An integrated approach: managing resources for post-disaster reconstruction." *Disasters*, 35(4), 739–765.

Cimellaro, G. P., Reinhorn, A. M., and Bruneau, M. (2010). "Framework for analytical quantification of disaster resilience." *Engineering Structures*, Elsevier Ltd, 32(11), 3639–3649.

Clark, C. E. (1962). "The PERT model for the distribution of an activity time." *Operations Research*, INFORMS, 10(3), 405–406.

Comerio, M. C. (2016). "Disaster Recovery and Community Adaption." *2016 NZSEE Conference*.

Cook, D. T., Liel, A. B., Haselton, C. B., and Koliou, M. (2022). "A framework for operationalizing the assessment of post-earthquake functional recovery of buildings." *Earthquake Spectra*, SAGE Publications Sage UK: London, England, 87552930221081540.

Danziger, M. M., and Barabási, A.-L. (2022). "Recovery coupling in multilayer networks." *Nature Communications*, 13(1), 955.

Davidson, C. H., Johnson, C., Lizarralde, G., Dikmen, N., and Sliwinski, A. (2007). "Truths and myths about community participation in post-disaster housing projects." *Habitat International*, 31(1), 100–115.

Didier, M., Grauvogl, B., Steentoft, A., Ghosh, S., and Stojadinović, B. (2017). "Seismic resilience of the Nepalese power supply system during the 2015 Gorkha earthquake." *16th World Conference on Earthquake Engineering, Santiago, Chile, 9-13 January.*, (May).

Dueñas-Osorio, L., and Kwasinski, A. (2012). "Quantification of lifeline system interdependencies after the 27 February 2010 Mw 8.8 offshore Maule, Chile, earthquake." *Earthquake Spectra*, 28(SUPPL.1), 581–603.

Dueñas-Osorio, L., Craig, J. I., and Goodno, B. J. (2007). "Seismic response of critical interdependent networks." *Earthquake engineering & structural dynamics*, Wiley Online Library, 36(2), 285–306.

FEMA. (2003). *HAZUS MR4 multi-hazard loss estimation methodology – earthquake model – technical manual*.

FEMA. (2012). *Seismic performance assessment of buildings: FEMA P58 guidelines*. Redwood City, California.

FEMA. (2022). “Hazus Earthquake Model Technical Manual Hazus 5.1.” Federal Emergency Management Agency (FEMA).

Gao, X., Barabady, J., and Markeset, T. (2010). “An approach for prediction of petroleum production facility performance considering Arctic influence factors.” *Reliability Engineering & System Safety*, 95(8), 837–846.

Gautam, D., Adhikari, R., and Rupakhety, R. (2021). “Seismic fragility of structural and non-structural elements of Nepali RC buildings.” *Engineering Structures*, 232, 111879.

Gharaati, M., and Davidson, C. (2008). “Who knows best? An overview of reconstruction after the earthquake in Bam, Iran.” *Proceedings of the Fourth International Conference 2008 Building resilience: achieving effective post-disaster reconstruction*, Canterbury, New Zealand, 13.

Giordano, N., Norris, A., Manandhar, V., Shrestha, L., Paudel, D. R., Quinn, N., Rees, E., Shrestha, H., Marasini, N. P., Prajapati, R., Guragain, R., De Luca, F., and Sextos, A. (2021). “Financial assessment of incremental seismic retrofitting of Nepali stone-masonry buildings.” *International Journal of Disaster Risk Reduction*, 60, 102297.

Goldratt, E. (1997). *Critical Chain*. The North River Press, MA.

Gondia, A., Siam, A., El-Dakhakhni, W., and Nassar, A. H. (2020). “Machine Learning Algorithms for Construction Projects Delay Risk Prediction.” *Journal of Construction Engineering and Management*, 146(1).

Guidotti, R., Chmielewski, H., Unnikrishnan, V., Gardoni, P., McAllister, T., and van de Lindt, J. (2016). “Modeling the resilience of critical infrastructure: the role of network dependencies.” *Sustainable and Resilient Infrastructure*, 1(3–4), 153–168.

Hajdu, M. (2013). “Effects of the application of activity calendars on the distribution of project duration in PERT networks.” *Automation in Construction*, 35, 397–404.

He, X., and Cha, E. J. (2018). “Modeling the damage and recovery of interdependent critical infrastructure systems from natural hazards.” *Reliability Engineering & System Safety*, 177, 162–175.

Huang, C., and Galasso, C. (2019). “Ground-motion intensity measure correlations observed in Italian strong-motion records.” *Earthquake Engineering & Structural Dynamics*, Wiley Online Library, 48(15), 1634–1660.

Hwang, C.-L., and Yoon, K. (1981). *Multiple Attribute Decision Making*. Lecture Notes in Economics and Mathematical Systems, Springer Berlin Heidelberg, Berlin, Heidelberg.

IOM. (2015). *Haiti — Earthquake Displacement Report 22 (March 2015)*.

Jahn, I. R., Guadagno, L., Gandia, E., and Bonnefoy, V. (2017). “Overcoming Land Tenure Barriers in Shelter and Other Reconstruction Activities in Post-disaster Settings.” *Identifying Emerging Issues in Disaster Risk Reduction, Migration, Climate Change and Sustainable Development*, Springer International Publishing, Cham, 161–176.

Jenkins, L. T., Creed, M. J., Tarbali, K., Muthusamy, M., Trogrlić, R. Š., Phillips, J. C., Watson, C. S., Sinclair, H. D., Galasso, C., and McCloskey, J. (2023). “Physics-based simulations of multiple natural hazards for risk-sensitive planning and decision making in expanding urban regions.” *International Journal of Disaster Risk Reduction*, 84, 103338.

Johansen, C., and Tien, I. (2018). “Probabilistic multi-scale modeling of interdependencies between critical infrastructure systems for resilience.” *Sustainable and Resilient*

Infrastructure, Taylor & Francis, 3(1), 1–15.

Kammouh, O., Gardoni, P., and Cimellaro, G. P. (2020). “Probabilistic framework to evaluate the resilience of engineering systems using Bayesian and dynamic Bayesian networks.” *Reliability Engineering & System Safety*, 198, 106813.

Karunasena, G., and Rameezdeen, R. (2010). “Post-disaster housing reconstruction.” *International Journal of Disaster Resilience in the Built Environment*, 1(2), 173–191.

Keefer, D. L., and Verdini, W. A. (1993). “Better estimation of PERT activity time parameters.” *Management science*, INFORMS, 39(9), 1086–1091.

Kennedy, J., Ashmore, J., Babister, E., and Kelman, I. (2008). “The meaning of ‘build back better’: evidence from post-tsunami Aceh and Sri Lanka.” *Journal of contingencies and crisis management*, Wiley Online Library, 16(1), 24–36.

Kuehn, N. M., and Abrahamson, N. A. (2020). “Spatial correlations of ground motion for non-ergodic seismic hazard analysis.” *Earthquake Engineering & Structural Dynamics*, Wiley Online Library, 49(1), 4–23.

Li, Z., Jin, C., Hu, P., and Wang, C. (2019). “Resilience-based transportation network recovery strategy during emergency recovery phase under uncertainty.” *Reliability Engineering & System Safety*, 188, 503–514.

Lin, P., and Wang, N. (2017a). “Stochastic post-disaster functionality recovery of community building portfolios II: Application.” *Structural Safety*, 69, 106–117.

Lin, P., and Wang, N. (2017b). “Stochastic post-disaster functionality recovery of community building portfolios I: Modeling.” *Structural Safety*, 69, 96–105.

Liu, W., Song, Z., Ouyang, M., and Li, J. (2020). “Recovery-based seismic resilience enhancement strategies of water distribution networks.” *Reliability Engineering & System Safety*, 203, 107088.

Markhvida, M., Ceferino, L., and Baker, J. W. (2018). “Modeling spatially correlated spectral accelerations at multiple periods using principal component analysis and geostatistics.” *Earthquake Engineering & Structural Dynamics*, 47(5), 1107–1123.

Martins, L., and Silva, V. (2021). “Development of a fragility and vulnerability model for global seismic risk analyses.” *Bulletin of Earthquake Engineering*, 19(15), 6719–6745.

Mensah, A. F., and Dueñas-Osorio, L. (2016). “Efficient Resilience Assessment Framework for Electric Power Systems Affected by Hurricane Events.” *Journal of Structural Engineering*, 142(8), 1–10.

Miyamjima, M., Fallahi, A., Ikemoto, T., Samaei, M., Karimzadeh, S., Setiawan, H., Talebi, F., and Karashi, J. (2018). “Site Investigation of the Sarpole-Zahab Earthquake, Mw 7.3 in SW Iran of November 12, 2017.” *JSCE Journal of Disaster FactSheets*, (June).

nPlan. (2022). “The State of Project Delivery 2022.” <https://app.hubspot.com/documents/8346925/view/486941752?accessId=71f89e> (Aug. 16, 2023).

Opabola, E. A., Elwood, K. J., and Liel, A. B. (2021). “Evaluation of seismic performance of as-built and retrofitted reinforced concrete frame structures with LAP splice deficiencies.” (January), 1–22.

Opabola, E. A., and Galasso, C. (2022). “Multicriteria decision making for selecting an optimal survey approach for large building portfolios.” *International Journal of Disaster*

Risk Reduction, 76, 102985.

Opabola, E. A., Galasso, C., Rossetto, T., Meilianda, E., Idris, Y., and Nurdin, S. (2023). "Investing in disaster preparedness and effective recovery in school physical infrastructures." *International Journal of Disaster Risk Reduction*, 103623.

Ophiyandri, T., Amaratunga, D., Pathirage, C., and Keraminiyage, K. (2013). "Critical success factors for community-based post-disaster housing reconstruction projects in the pre-construction stage in Indonesia." *International Journal of Disaster Resilience in the Built Environment*, 4(2), 236–249.

Ouyang, M., and Dueñas-Osorio, L. (2014). "Multi-dimensional hurricane resilience assessment of electric power systems." *Structural Safety*, 48, 15–24.

Pan, X., Dang, Y., Wang, H., Hong, D., Li, Y., and Deng, H. (2022). "Resilience model and recovery strategy of transportation network based on travel OD-grid analysis." *Reliability Engineering & System Safety*, 223, 108483.

Peacock, W. G., Van Zandt, S., Zhang, Y., and Highfield, W. E. (2014). "Inequities in Long-Term Housing Recovery After Disasters." *Journal of the American Planning Association*, 80(4), 356–371.

Resio, D. T., Irish, J., and Cialone, M. (2009). "A surge response function approach to coastal hazard assessment – part 1: basic concepts." *Natural Hazards*, 51(1), 163–182.

Saaty, T. L. (1980). *The Analytic Hierarchy Process: Planning, Priority Setting, Resource Allocation*. McGraw-Hill International Book Co., New York; London.

Samaratunge, R., Coghill, K., and Herath, H. M. A. (2012). "Governance in Sri Lanka: Lessons from Post-Tsunami Rebuilding." *South Asia: Journal of South Asian Studies*, 35(2), 381–407.

Shafique, K., and Warren, C. M. J. (2015). "Significance of community participation in success of post natural disaster reconstruction project–evidence from developing country." *5th International Conference on Building Resilience*, 1–12.

Sharma, K., Apil, K. C., Subedi, M., and Pokharel, B. (2018). "Challenges for reconstruction after M w 7.8 gorkha earthquake: A study on a devastated area of Nepal." *Geomatics, Natural Hazards and Risk*, Taylor & Francis, 9(1), 760–790.

Sharma, N., and Gardoni, P. (2022). "Mathematical modeling of interdependent infrastructure: An object-oriented approach for generalized network-system analysis." *Reliability Engineering & System Safety*, 217, 108042.

Shinozuka, M., Chang, S. E., Cheng, T.-C., Feng, M., O'rourke, T. D., Saadeghvaziri, M. A., Dong, X., Jin, X., Wang, Y., and Shi, P. (2004). *Resilience of integrated power and water systems*. Citeseer.

Shinozuka, M., Dong, X., Chen, T. C., and Jin, X. (2007). "Seismic performance of electric transmission network under component failures." *Earthquake engineering & structural dynamics*, Wiley Online Library, 36(2), 227–244.

Van Slyke, R. M. (1963). "Monte Carlo Methods and the PERT Problem." *Operations Research*, 11(5), 839–860.

Stewart, J. P., Douglas, J., Javanbarg, M., Bozorgnia, Y., Abrahamson, N. A., Boore, D. M., Campbell, K. W., Delavaud, E., Erdik, M., and Stafford, P. J. (2015). "Selection of Ground Motion Prediction Equations for the Global Earthquake Model." *Earthquake Spectra*, 31(1), 19–45.

Straub, D., and Der Kiureghian, A. (2008). "Improved seismic fragility modeling from empirical data." *Structural safety*, Elsevier, 30(4), 320–336.

Tas, N., Tas, M., and Cosgun, N. (2011). "Permanent housing production process after 17 August 1999 Marmara Earthquake in Turkey." *International Journal of Strategic Property Management*, Taylor & Francis, 15(3), 312–328.

Terzic, V., Villanueva, P. K., Saldana, D., and Yoo, D. Y. (2021). "Framework for modelling post-earthquake functional recovery of buildings." *Engineering Structures*, Elsevier Ltd, 246(September 2020), 113074.

The Asia Foundation. (2016). "Nepal Government Distribution of Earthquake Reconstruction Cash Grants for Private Houses." IRM—Thematic Study San Francisco.

UNDP. (2021). "2021/22 HDR Technical Notes."

Unnikrishnan, V. U., and van de Lindt, J. W. (2016). "Probabilistic framework for performance assessment of electrical power networks to tornadoes." *Sustainable and Resilient Infrastructure*, Taylor & Francis, 1(3–4), 137–152.

Vanzi, I. (2000). "Structural upgrading strategy for electric power networks under seismic action." *Earthquake engineering & structural dynamics*, Wiley Online Library, 29(7), 1053–1073.

Villar-Vega, M., Silva, V., Crowley, H., Yepes, C., Tarque, N., Acevedo, A. B., Hube, M. A., Gustavo, C. D., and María, H. S. (2017). "Development of a fragility model for the residential building stock in South America." *Earthquake Spectra*, SAGE Publications Sage UK: London, England, 33(2), 581–604.

Waheeb, R. A., and Andersen, B. S. (2022). "Causes of Problems in Post-Disaster

Emergency Re-Construction Projects—Iraq as a Case Study." *Public Works Management & Policy*, 27(1), 61–97.

Wang, W. (Lisa), and van de Lindt, J. W. (2021). "Quantitative modeling of residential building disaster recovery and effects of pre- and post-event policies." *International Journal of Disaster Risk Reduction*, 59, 102259.

Weerakoon, D., Jayasuriya, S., Arunatilake, N., and Steele, P. (2007). *Economic challenges of post-tsunami reconstruction in Sri Lanka*. ADBI Discussion Paper.

Westoby, L., Wilkinson, S., and Dunn, S. (2021). "The road to recovery: Understanding the challenges affecting school reconstruction in rural Nepal following the 2015 Gorkha earthquake." *International Journal of Disaster Risk Reduction*, Elsevier Ltd, 56(February), 102120.

Wu, Y., and Chen, S. (2023). "Resilience modeling and pre-hazard mitigation planning of transportation network to support post-earthquake emergency medical response." *Reliability Engineering & System Safety*, 230, 108918.

Xiao, Y., Zhao, X., Wu, Y., Chen, Z., Gong, H., Zhu, L., and Liu, Y. (2022). "Seismic resilience assessment of urban interdependent lifeline networks." *Reliability Engineering & System Safety*, 218, 108164.

Yu, Y.-C., and Gardoni, P. (2022). "Predicting road blockage due to building damage following earthquakes." *Reliability Engineering & System Safety*, 219, 108220.

Zou, Q., and Chen, S. (2021). "Resilience-based Recovery Scheduling of Transportation Network in Mixed Traffic Environment: A Deep-Ensemble-Assisted Active Learning Approach." *Reliability Engineering & System Safety*, 215, 107800.

9 AUTHOR CONTRIBUTIONS

EO: Conceptualization; Data curation; Formal Analysis; Methodology; Writing – original draft; Writing – review & editing
CG: Conceptualization; Writing – original draft; Writing – review & editing

We the undersigned declare that this manuscript is original, has not been published before and is not currently being considered for publication elsewhere.

We confirm that the manuscript has been read and approved by all named authors and that there are no other persons who satisfied the criteria for authorship but are not listed. We further confirm that the order of authors listed in the manuscript has been approved by all of us.

Declaration of interests

☒ The authors declare that they have no known competing financial interests or personal relationships that could have appeared to influence the work reported in this paper.

☐ The authors declare the following financial interests/personal relationships which may be considered as potential competing interests: